

# Self-assembling processes involved in the molecular beam epitaxy growth of stacked InAs/InP quantum wires

J M Ulloa , P M Koenraad , D Fuster , L González , Y González  
and M U González

Department of Applied Physics, Eindhoven University of Technology, PO Box 513,  
NL-5600MB Eindhoven, The Netherlands

Instituto de Microelectrónica de Madrid (CNM-CSIC), Isaac Newton 8, 28760 Tres Cantos,  
Madrid, Spain

## Abstract

The growth mechanism of stacked InAs/InP(001) quantum wires (QWRs) is studied by combining an atomic-scale cross-sectional scanning tunnelling microscopy analysis with *in situ* and in real-time stress measurements along the [110] direction (sensitive to stress relaxation during QWR formation). QWRs in stacked layers grow by a non-Stranski-Krastanov (SK) process which involves the production of extra InAs by strain-enhanced As/P exchange and a strong strain driven mass transport. Despite the different growth mechanism of the QWR between the first and following layers of the stack, the QWRs maintain on average the same shape and composition in all the layers of the stack, revealing the high stability of this QWR configuration.

## 1. Introduction

The growth of stacked layers is a common approach to improve the spatial distribution and size homogeneity of self-assembled nanostructures . Stacking nanostructures leads to a vertical correlation between the different layers depending on the spacer layer thickness. This is due to the strain fields produced by the buried nanostructures that propagate towards the capping layer surface where the next layer of nanostructures will be formed . The vertical stacking of self-assembled InAs quantum wires (QWRs) grown on InP(001) has a particular interest since they emit light at 1.55  $\mu\text{m}$ . These QWRs are formed instead of quantum dots due to a strong stress anisotropy built up during the growth process: the stress is much higher along the [110] direction than along the  $\bar{[110]}$  direction. This is due to the distortion of As-In bonds along [110] and As-As dimerization along  $\bar{[110]}$ . Therefore, stress relaxation takes place mainly along the [110] direction and the resulting nanostructures are elongated (typically more than 1  $\mu\text{m}$  long) along the [110] direction. In the case of InAs/InP QWR stacking, the presence of strain

in the growth front can lead to relevant differences between the stacked layers and the first one. In a previous work, it was demonstrated that an extra amount of InAs is incorporated with respect to the amount of InAs that is deposited when the stacked QWR layers are separated by thin InP spacer layers ( $d < 10 \text{ nm}$ ) . Consequently, differences in size, shape or composition between the first and the stacked layers could be expected. According to those results, the formation of QWRs in correlated stacked layers could be explained by considering a combination of strain driven mass transport together with an efficient As/P exchange.

In this work, we have focused on getting a deeper insight in the formation process of correlated layers of QWRs by combining an atomic-scale cross-sectional scanning tunnelling microscopy (X-STM) study with *in situ* and real-time stress measurements along the [110] direction (sensitive to stress relaxation during QWR formation). Contrary to expectations, we have found a strong stability in the size, shape and composition of the QWRs in the different layers. Despite that, we have been able to explain the distribution of the extra amount of InAs incorporated in the stacked QWR layers

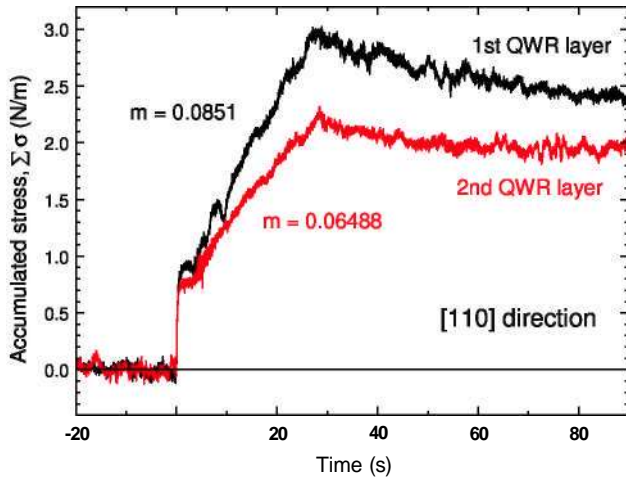


**Figure 1.** Accumulated stress ( $\Sigma\sigma$ ) along the [110] direction during InAs deposition for the growth of two stacked QWR layers separated by 5 nm of InP. Despite the higher amount of InAs formed with respect to the InAs deposited (see text), the slope ( $m$ ) is smaller in the second layer, indicating that stress is being relaxed from the onset of InAs growth.

separated by a thin InP layer. Having revealed the processes underlying the formation of nanostructures in stacked layers, our results permit us to demonstrate the prediction that the nanostructure formation process is different under the presence of strain, as proposed in previous works

## 2. Experimental details

The analysed samples consist of three stacked layers of InAs QWRs grown on InP(OOI) substrates by solid-source molecular beam epitaxy (MBE) and separated by 5 nm thick InP spacer layers. The QWRs were formed by depositing 2.5 monolayers (ML) of InAs at  $0.1 \text{ ML s}^{-1}$  at a growth temperature of  $515 \text{ }^\circ\text{C}$  and a beam equivalent pressure ( $P_{\text{As4}} = 2.3 \times 10^{-6} \text{ mbar}$ ). The InP spacer layer was grown at  $380 \text{ }^\circ\text{C}$  by atomic layer MBE at  $1 \text{ ML s}^{-1}$ . The resulting QWRs are oriented along [110] and periodically arranged along the [110] direction

The evolution of stress in the [110] direction during QWR formation was obtained by optical monitoring of the substrate curvature. This technique provides an *in situ* and real-time measurement of the film accumulated stress ( $\Sigma\sigma$ ) (stress

integrated along the layer thickness). The X-STM measurements were performed at room temperature on the (110) surface plane of *in situ* cleaved samples under UHV ( $p < 4 \times 10^{-11} \text{ Torr}$ ) conditions. All the images shown in this paper were obtained in constant current mode at negative voltage (filled states) so the group V elements (As and P) are directly imaged.

## 3. Results

As studied previously, the evolution of  $\Sigma\sigma$  during InAs growth on InP shows a different behaviour in the two (110) directions. However, in both directions the evolution of  $\Sigma\sigma$  shows a linear increase with the same slope corresponding to pseudomorphic growth; that is, the InAs layer is growing bi-dimensionally and coherently on the substrate. These results concern the growth of a single layer of QWRs or the first layer in a stack. However, in correlated stacked QWR layers, the linear increase in  $\Sigma\sigma$  takes place with different slopes in both directions.

Along [110] the larger slope of  $\Sigma\sigma$  for the second grown QWR layer is due to an actual increase of InAs incorporated in the wires compared to the deposited amount. This increase in effective InAs growth rate should also result in an increase in  $\Sigma\sigma$  measured along [110]. However, we observe exactly the opposite: an evident decrease in the  $\Sigma\sigma$  slope with respect to that observed during the growth of InAs in the first QWR layer (see figure 1). This effect can only be due to the appearance of structures capable of relaxing the stress in this direction, demonstrating that, in correlated layers, QWR formation starts at the beginning of InAs deposition. This non-SK growth was predicted, pointing out that the concept of a critical thickness of a bi-dimensional strained layer needed for nanostructure formation, as in an SK process, is no longer applicable in the case of correlated QWR layers from the second layer on.

The results presented reveal the behaviour of the QWR formation process in single layers as well as in correlated layers where strain profiles are present at the growth front. An atomistic insight into the differences between these two cases can be extracted from X-STM measurements. Figure 2 shows a filled states image of the three QWR layers. The QWRs in cross-section are generally triangular (sometimes trapezoidal),

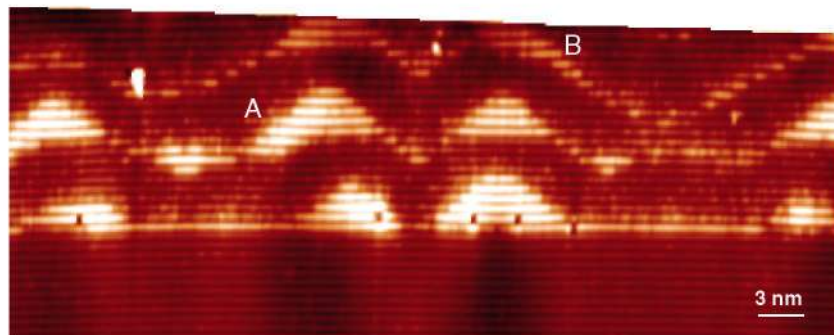


**Figure 2.** Filled states image of the three QWR layers. The bright spots are As atoms in the InP matrix. The shapes of QWR A and QWR B evidence the asymmetric shape due to non-SK QWR formation above the first layer of the stack.

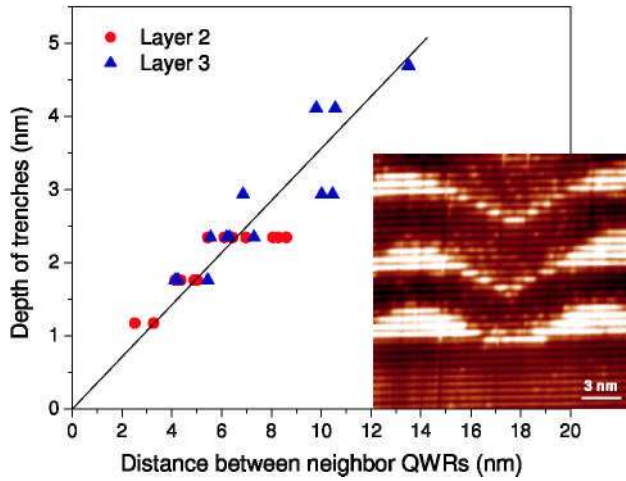


**Figure 3.** Depth of the trenches as a function of the distance between neighbouring QWRs in the second and third layers of the stack. The linear fit indicates an angle of  $35^\circ$  with the growth surface. The inset shows a filled states image of two trenches, showing that they are parallel.

with an average height of  $\sim 3$  nm. Remarkably, triangular trenches with different depths can always be observed between QWRs in the second and third layers. The InP growth surface is flat before the second QWR layer is deposited, as observed by atomic force microscopy in a similar sample in which the growth was stopped at that point. Therefore, the trenches must be created by a process of excavating of the InP spacer layer due to As/P exchange and strain driven mass transport,

From figure 2, and the inset in figure 3, it can also be observed that the trenches are not rounded as previously observed for InAs/InP quantum dots (QDs), but they are perfectly triangular with always a similar angle of about  $\sim 30^\circ$  to  $40^\circ$  to the original surface. Surprisingly, the angle coincides nicely with those of the QWR facets. Figure 3 shows the depth of the trenches as a function of the distance between neighbouring QWRs. The trenches are on average deeper in the third layer, due to the higher accumulated strain. The depth clearly increases with the distance between QWRs. The linear fit gives an angle of  $35^\circ$ , which corresponds to the (112) and (112) facets. Therefore, as a result of the As/P exchange process the same {112} facets (making  $\sim 35^\circ$  with the growth surface) are always created between QWRs, which means that the exchange process will continue creating extra InAs until those stable facets are created, and at that point the exchange process will stop. The production of extra InAs through As/P exchange is consequently a self-limited process in this case. When the QWRs are very close, the stable facets will form a shallow trench, while the resulting trench formed by the same facets will be deeper if the QWRs are far away from each other (see figure 4). This will give rise to an asymmetric mass transport to the QWRs, resulting in significantly different trenches on both sides of the QWR, which can result in the formation of asymmetric QWRs. Examples of that can be observed in figure 2 in the second layer (QWR A) and in the third layer (QWR B).

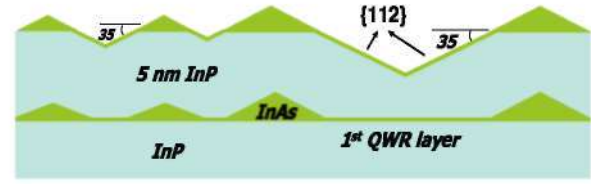


**Figure 4.** Schematic description of the first and second QWR layers separated by a 5 nm thick InP spacer layer. The growth process will stop when the stable facets making  $\alpha \cong 35^\circ$  with the growth surface ({112} facets) are formed. Consequently, the depth of the resulting trenches increases with the distance between QWRs.

The same amount of InAs was deposited in all three QWR layers. Because a lot of extra InAs is produced by As/P exchange in the second and third layers, a considerable difference in size and/or composition is to be expected between the QWRs in the first layer formed by an SK growth mode and the other ones. Analysing the size of the QWRs in the different layers of the stack, we have found the average area of the cross-section of the QWRs to be  $13.8 \pm 0.8$  nm<sup>2</sup>,  $14.0 \pm 1.1$  nm<sup>2</sup> and  $11.0 \pm 1.2$  nm<sup>2</sup> for layers 1, 2 and 3, respectively. Thus, surprisingly, the QWRs in the second and third layers are not bigger than those in the first one, and thus the size of the QWRs does not reflect the presence of the extra InAs. It is possible that this can be explained by a change in the composition of the QWRs in the different layers of the stack. The composition of the QWRs was investigated by analysing the atomically resolved filled states images, in which the As and P atoms can be distinguished. In figure 5(a), the As atoms in the InP matrix appear as bright features and the P atoms in InAs appear as dark spots. As shown in figure 5(a), only a few P atoms can be observed inside the QWRs (in particular four in QWR A and two in QWR B), indicating that the composition is close to 100% InAs in every case. This result is confirmed by analysing the strain in the nanostructures. Due to the compressive strain, the surface will relax outwards after cleavage in the QWR regions. This outward relaxation can be directly measured by X-STM by scanning at high negative voltages ( $\sim -3.0$  V). The relaxation profile of a QWR in the first layer was compared to calculations from continuum elasticity theory. A finite element calculation was performed to solve the 3D problem, in which the size and shape of the QWR were extracted from the measurements and the composition was changed to fit the measured outward relaxation profile. Figure 5(b) shows the measured outward relaxation profile and the calculated one when the QWR is considered to be 100% InAs. The good fit confirms that the QWRs in the first layer are close to 100% InAs, and the same is obtained for the QWRs in the other two layers. Therefore, differences in composition cannot explain the presence of extra InAs. The amount of As in the InP barrier above the first layer and the others is very similar (see figure 5(a)), so the higher amount of As in the capping layer in the second and third layers must also be ruled out as an explanation.

As described, the extra InAs produced by strain-enhanced As/P exchange in the second and third layers does not give rise to bigger or As-rich QWRs. We conclude that part of the

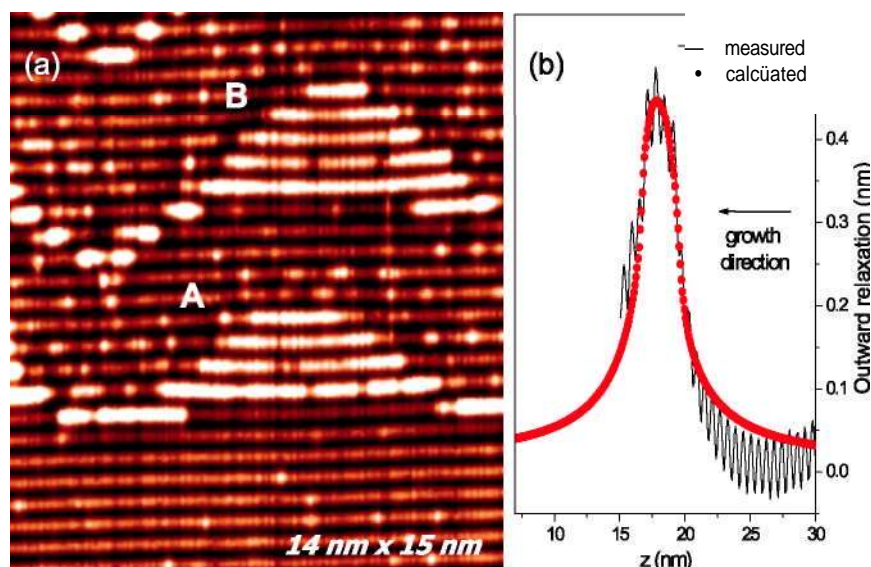


**Figure 5.** (a) Filled states image treated with a local mean equalization filter showing two QWRs in the first and second layers (QWR A and QWR B, respectively). The dark spots inside the QWRs are single P atoms. (b) Measured and calculated outward relaxation profile through the middle of a QWR in the first layer.

extra InAs material due the As/P exchange process is involved in creating the asymmetric regions of some QWRs as we have shown above. Note that these regions were not included in the size measurements from which the average area of the QWR was determined. The other part of the extra InAs is accumulated in the trenches, creating inverted QWRs or QDs (see figure 2). Finally, a large amount of the extra InAs is found to be creating a few big QWRs formed by the overlapping of two or more normal QWRs. In particular, in the third layer a very few huge QWRs with a cross-sectional area which is two orders of magnitude bigger than the average value are observed, compensating for the smaller average area found in the QWRs of that layer.

#### 4. Conclusión

In conclusión, X-STM was used together with *in situ* stress measurements along the [110] direction to investigate the growth mechanism of stacked InAs/InP(001) QWRs. The results obtained demonstrate that the QWR formation process of the first and the other layers of the stack is drastically different. While QWRs in the first layer form by an SK process, the stacked QWRs start to form as soon as the P flux is changed to As flux. This growth mechanism involves a self-limited production of extra InAs by As/P exchange and a strong mass transport. Nevertheless, the structural properties of the average QWRs in the different layers remain quite similar, indicating the high stability of this QWR configuration.

#### Acknowledgments

This work has been supported by the European Union through the SANDiE Network of Excellence (contract No. NMP4-CT-2004-500101). The authors also acknowledge financial support

by the Spanish MEC and CAM through projects TEC-2005-05781-C03-01, NAN2004-09109-C04-01, Consolider QOIT CSD2006-0019 and S-505/ESP/000200.

#### References

- Xie Q, Madhukar A, Chen P and Kobayashi N P 1995 *Phys. Rev. Lett.* **75** 2542
- Tersoff J, Teichert C and Lagally M G 1996 *Phys. Rev. Lett.* **76** 1675
- Heitz R, Kalburge A, Xie Q, Grundmann M, Chen P, Hoffmann A, Madhukar A and Bimberg D 1998 *Phys. Rev. B* **57** 9050
- Lita B, Goldman R S, Philips J D and Bhattacharya P K 1999 *Appl. Phys. Lett.* **74** 2824
- Alen B, Martínez-Pastor J, González L, García J M, Molina S I, Ponce A and García R 2002 *Phys. Rev. B* **65** 241301
- García J M, González L, González M U, Silveira J P, González Y and Briones F 2001 *J. Cryst. Growth* **227** 975
- Fuster D, González M U, González L and González Y 2004 *Appl. Phys. Lett.* **84** 4723
- González L, García J M, García R, Briones F, Martínez-Pastor J and Ballesteros C 2000 *Appl. Phys. Lett.* **76** 1104
- Volkert C A 1991 *J. Appl. Phys.* **70** 3521
- González M U, González Y and González L 2002 *Appl. Phys. Lett.* **81** 4162
- González M U, González L, García J M, González Y, Silveira J P and Briones F 2004 *Microelectron. J.* **35** 13
- Gutiérrez H R, Cotta M A, Bortoleto J R R and de Carvalho M M G 2002 *J. Appl. Phys.* **92** 7523
- Ouattara L, Mikkelsen A, Lundgren E, Borgström M, Samuelson L and Seifert W 2004 *Nanotechnology* **15** 1701
- Ulloa J Metal 2007 *J. Appl. Phys.* **101** 081707
- Feenstra R M 1999 *Physica B* **273** 796
- Bruls D M, Vugs J W A M, Koenraad P M, Salemink H W M, Wolter J H, Hopkinson M, Skolnick M S, Long F and Gilí S P A 2002 *Appl. Phys. Lett.* **81** 1708